Steel and Composite Structures, *Vol. 30, No. 2 (2019) 109-121*
DOI: https://doi.org/10.12989/scs.2019.30.2.109

Modeling for the strap combined footings Part II: Mathematical model for design

Juan Antonio Yáñez-Palafox [a], Arnulfo Luévanos-Rojas [*], Sandra López-Chavarría [b] and Manuel Medina-Elizondo [c]

Institute of Multidisciplinary Researches, Autonomous University of Coahuila, Blvd. Revolución No, 151 Ote, CP 27000, Torreón, Coahuila, México

(*Received May 3, 2018, Revised December 20, 2018, Accepted January 16, 2019*)

Abstract. This paper presents the second part of the modeling for the strap combined footings, this part shows a mathematical model for design of strap combined footings subject to axial load and moments in two directions to each column considering the soil real pressure acting on the contact surface of the footing for one and/or two property lines of sides opposite restricted, the pressure is presented in terms of an axial load, moment around the axis "X" and moment around the axis "Y" to each column, and the methodology is developed using the principle that the derived of the moment is the shear force. The first part shows the optimal contact surface for the strap combined footings to obtain the most economical dimensioning on the soil (optimal area). The classic model considers an axial load and a moment around the axis "X" (transverse axis) applied to each column, i.e., the resultant force from the applied loads is located on the axis "Y" (longitudinal axis), and its position must match with the geometric center of the footing, and when the axial load and moments in two directions are presented, the maximum pressure and uniform applied throughout the contact surface of the footing is considered the same. A numerical example is presented to obtain the design of strap combined footings subject to an axial load and moments in two directions applied to each column. The mathematical approach suggested in this paper produces results that have a tangible accuracy for all problems and it can also be used for rectangular and T-shaped combined footings.

Keywords: mathematical model for design; strap combined footings; moments; bending shear; punching shear

1. Introduction

The distribution of soil pressure under a footing is a function of the type of soil, the relative rigidity of the soil and the footing, and the depth of foundation at level of contact between footing and soil. A concrete footing on sand will have a pressure distribution similar to Fig. 1(a). When a rigid footing is resting on sandy soil, the sand near the edges of the footing tends to displace laterally when the footing is loaded. This tends to decrease in soil pressure near the edges, whereas soil away from the edges of footing is relatively confined. On the other hand, the pressure distribution under a footing on clay is similar to Fig. 1(b). As the footing is loaded, the soil under the footing deflects in a bowl-shaped depression, relieving the pressure under the middle of the footing. However, for the sake of simplicity the footing is assumed to be a perfectly rigid body, the soil is assumed to behave elastically and the distributions of stress and strain are linear in the soil just below the base of the foundation. Therefore for design purposes, it is common to assume the soil pressures are linearly distributed. The pressure distribution will be uniform if the centroid of the footing coincides with the resultant of the applied loads, as shown in Fig. 1(c) (Bowles 2001).

Construction practice may dictate using only one footing for two or more columns due to: (1) Closeness of column (for example around elevator shafts and escalators); (2) Due to property line constraint, this may limit the size of footings at boundary. The eccentricity of a column placed on an edge of a footing may be compensated by tying the footing to the interior column.

The hypothesis used in the classical model considers an axial load and a moment around the axis "X" (transverse axis) applied to each column, i.e., the resultant force from the applied loads is located on the axis "Y" (longitudinal axis), and its position must match with the geometric center

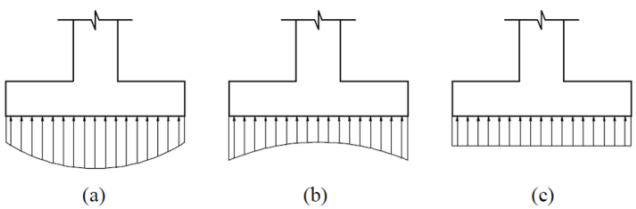

Fig. 1 Pressure distribution under footing; (a) footing on sand; (b) footing on clay; (c) equivalent uniform distribution

*Corresponding author, Ph.D.,
E-mail: arnulfol_2007@hotmail.com
[a] Ph.D. Candidate, E-mail: jayp.ep@gmail.com
[b] Ph.D., E-mail: sandylopez5@hotmail.com
[c] Ph.D., E-mail: drmanuelmediana@yahoo.com.mx

ISSN: 1229-9367 (Print), 1598-6233 (Online)

of the footing, and when the axial load and moments in two directions are presented, the maximum pressure and uniform applied throughout the contact surface of the footing is considered the same. Then the equation of the biaxial bending is used to obtain the stresses acting on the contact surface of the combined footings, which must meet the following conditions: (1) The minimum stress should be equal to or greater than zero, because the soil is not capable of withstand tensile stresses; (2) The maximum stress must be equal or less than the allowable capacity that can withstand the soil (Das *et al*. 2006, Bowles 2001, Calavera-Ruiz 2000, Tomlinson 2008).

Many researchers in the past have been investigated foundation structures or structural footings and the main papers are: Response of a rectangular plate-column system on a tensionless Winkler foundation subjected to static and dynamic loads (Guler and Celep 2005); Nonlinear vibration of hybrid composite plates on elastic foundations (Chen *et al*. 2011); Performance-based framework for soil-structure systems using simplified rocking foundation models (Smith-Pardo 2011); Stochastic design charts for bearing capacity of strip footings (Shahin and Cheung 2011); Nonlinear analysis of finite beam resting on Winkler with consideration of beam-soil interface resistance effect (Zhang *et al*. 2011); Nonlinear interaction behaviour of infilled frame-isolated footings-soil system subjected to seismic loading (Agrawal and Hora 2012); Static response of 2-D functionally graded circular plate with gradient thickness and elastic foundations to compound loads (Rad 2012); Influence of inclusion of geosynthetic layer on response of combined footings on stone column reinforced earth beds (Maheshwari and Khatri 2012); Strenghtening and repair of concrete foundation beams whit fiber composite materials (Orbanich *et al*. 2012); Generalized Schmertmann Equation for settlement estimation of shallow footings in saturated and unsaturated sands (Mohamed *et al*. 2013); Design of isolated footings of rectangular form using a new model (Luévanos-Rojas *et al*. 2013); Analysis of elastic foundation plates with internal and perimetric stiffening beams on elastic foundations by using Finite Differences Method (Orbanich and Ortega 2013); Experimental estimate of Nγ values and corresponding settlements for square footings on finite layer of sand (Dixit and Patil 2013); The use of neural networks for the prediction of the settlement of pad footings on cohesionless soils based on standard penetration test (ErzÍn and Gul 2013); Decrease trends of ultimate loads of eccentrically loaded model strip footings close to a slope (Cure *et al*. 2014); Design of isolated footings of circular form using a new model (Luévanos-Rojas 2014a); Design of boundary combined footings of rectangular shape using a new model (Luévanos-Rojas 2014b); The bearing capacity of square footings on a sand layer overlying clay (Uncuoğlu 2015); Design of boundary combined footings of trapezoidal form using a new model (Luévanos-Rojas 2015); A comparative study for the design of rectangular and circular isolated footings using new models (Luévanos-Rojas 2016a); A new model for the design of rectangular combined footings of boundary with two opposite sides restricted (Luévanos-Rojas 2016b); Experimental and finite element analyses of footings of varying shapes on sand (Anil *et al*. 2017); A new mathematical model for design of square isolated footings for general case (López-Chavarría 2017); Pressure-settlement behavior of square and rectangular skirted footings resting on sand (Khatri *et al*. 2017); A comparative study for design of boundary combined footings of trapezoidal and rectangular forms using new models (Luévanos-Rojas *et al*. 2017); Bearing capacity of strip footings on a stone masonry trench in clay (Mohebkhah 2017); A new model for T-shaped combined footings Part II: Mathematical model for design (Luévanos-Rojas *et al*. 2018).

Thus, the review of the literature clearly shows that there is no close relationship with the topic of mathematical model of design for strap combined footings that is addressed in this paper.

The first part shows the optimal contact surface for strap combined footings to obtain the most economical dimensioning on the soil (optimal area). This paper presents the second part of a new mathematical model for strap combined footings to obtain the design of such foundations subject to an axial load and moments in two directions to each column considering the soil real pressure acting on the contact surface of the footing with one or two property lines restricted, the pressure is presented in terms of an axial load, moment around the axis "X" and moment around the axis "Y" to each column, and the methodology is developed using the principle that the derived of the moment is the shear force, and it is also considers as a single body the boundary footing, the inner footing and the strap beam (main objective of this investigation). To illustrate the validity of the new model, a numerical example is presented to obtain the design for strap combined footings subjected to an axial load and moments in two directions applied to each column.

2. Methodology

2.1 General conditions

According to Building Code Requirements for Structural Concrete (ACI 318S-14 2014) and Commentary the critical sections are: (1) the maximum moment is located in face of column, pedestal, or wall, for footings supporting a concrete column, pedestal, or wall; (2) bending shear is presented at a distance "*d*" (distance from extreme compression fiber to centroid of longitudinal tension reinforcement) shall be measured from face of column, pedestal, or wall for footings supporting a column, pedestal, or wall; (3) punching shear is localized so that it perimeter "b_o" is a minimum but need not approach closer than "*d*/*2*" to: (a) Edges or corners of columns, concentrated loads, or reaction areas; and (b) Changes in slab thickness such as edges of capitals, drop panels, or shear caps.

The general equation for any type of footings subjected to bidirectional bending (Luévanos-Rojas *et al*. 2013, Luévanos-Rojas 2014a, b, 2015, 2016a, b, Gere and Goodno 2009)

$$\sigma = \frac{P}{A} \pm \frac{M_x y}{I_x} \pm \frac{M_y x}{I_y} \tag{1}$$

where: σ is the stress exerted by the soil on the footing (soil pressure), A is the contact area of the footing, P is the axial load applied at the center of gravity of the footing, M_x is the moment around the axis "X", M_y is the moment around the axis "Y", x is the distance in the direction "X" measured from the axis "Y" to the fiber under study, y is the distance in direction "Y" measured from the axis "X" to the farthest under study, I_y is the moment of inertia around the axis "Y" and I_x is the moment of inertia around the axis "X".

2.2. New model for design of the strap combined footings

Fig. 3 of the Part 1 shows a strap combined footing under axial load and moment in two directions (biaxial bending) in each column, the pressure below the footing vary linearly (Luévanos-Rojas *et al*. 2013, Luévanos-Rojas 2014a, b, 2015, 2016a, b).

Fig. 4 of the Part 1 presents the diagram of pressure below the strap combined footing and also the stresses in each vertex.

The stresses anywhere of the contact surface the structural member due to the pressure that is exerted by the soil for the strap combined footing are obtained:

The stress in the main direction (axis "Y") is

$$\sigma(x,y)=\frac{R}{A}+\frac{M_{xT}y}{I_x}+\frac{M_{yT}x}{I_y} \tag{2}$$

where R, M_{xT}, M_{yT}, A, I_x and I_y are presented in Eqs. (14) to (21) of the part 1.

The stresses in the transverse direction to the main direction (axis "X") are:

To the number column 1 is

$$\sigma_{P_1}(x,y)=\frac{P_1}{w_1a_1}+\frac{12[M_{x1}+P_1(w_1-c_2)/2]y}{{w_1}^3a_1}+\frac{12M_{y1}x}{w_1{a_1}^3} \tag{3}$$

To the number column 2 is

$$\sigma_{P_2}(x,y)=\frac{P_2}{w_2b_1}+\frac{12[M_{x2}-P_2(w_2-c_4)/2]y}{{w_2}^3b_1}+\frac{12M_{y2}x}{w_2{b_1}^3} \tag{4}$$

where: w_1 and w_2 are the widths of the analysis surface for the columns 1 and 2 in the transverse direction to the main direction, these are: $w_1 = c_2 + d/2$, $w_2 = c_4 + d/2$ (column is located in the property line), $w_2 = c_4 + d$ (column is located in the center of the footing).

Geometry conditions are shown in Eqs. (22) to (24) of the part 1.

2.2.1 Moments

Critical sections for moments are presented in section a'-a', b'-b', c'-c', d'-d', e'-e', f'-f', g'-g' and h'-h', as shown in Fig. 2.

2.2.1.1 Moment around the axis y_1'- y_1' of $0 \le x_1 \le a_1/2$

Shear force "V_{x1}" is found through the volume of pressure the area formed by the axis y_1'- y_1' with a width "w_1" and the free end (left side of the Fig. 2) of the footing

$$V_{x_1}=-\int_{-w_1/2}^{w_1/2}\int_{x_1}^{a_1/2}\sigma_{P_1}(x,y)dxdy \tag{5}$$

$$V_{x_1}=\frac{6M_{y1}{x_1}^2}{{a_1}^3}+\frac{P_1x_1}{a_1}-\frac{P_1a_1+3M_{y1}}{2a_1} \tag{6}$$

If the derived of the moment is the shear force, therefore, it is presented as follows

$$V_{x_1}=\frac{dM_{y_1}{}'}{dx_1} \tag{7}$$

where: $M_{y1'}$ is the moment around the axis "y_1'" and V_{x1} is the shear force at a distance "x_1".

Now substituting Eq. (6) into Eq. (7) and integrating to obtain the moment in term of "x_1", this is presented as follows

$$M_{y_1'}=\frac{2M_{y1}{x_1}^3}{{a_1}^3}+\frac{P_1{x_1}^2}{2a_1}-\frac{P_1x_1}{2}-\frac{3M_{y1}x_1}{2a_1}+C_1 \tag{8}$$

Substituting "$x_1 = a_1/2$" and $M_{y1'} = 0$ into Eq. (8), the constant "C_1" is obtained

$$C_1=\frac{P_1a_1}{8}+\frac{M_{y1}}{2} \tag{9}$$

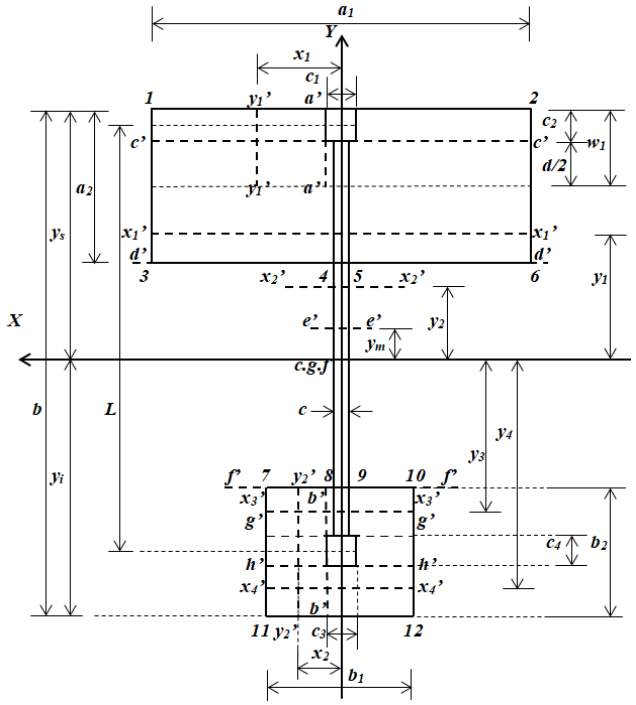

Fig. 2 Critical sections for moments

Now, substituting Eq. (9) into Eq. (8), the equation of moments is

$$M_{y_1'} = \frac{P_1(2x_1 - a_1)^2}{8a_1} + \frac{M_{y1}(4{x_1}^3 - 3{a_1}^2x_1 + {a_1}^3)}{2{a_1}^3} \quad (10)$$

Substituting "$x_1 = c_1/2$" into Eq. (10) to obtain "$M_{a'}$", this is

$$M_{a'} = \frac{\left[P_1{a_1}^2 + 2M_{y1}(2a_1 + c_1)\right](a_1 - c_1)^2}{8{a_1}^3} \quad (11)$$

2.2.1.2 Moment around the axis y_2'- y_2' of $0 \le x_2 \le b_1/2$

Shear force "V_{x2}" is found through the volume of pressure the area formed by the axis y_2'- y_2' with a width "w_2" and the free end (left side of the Fig. 2) of the footing

$$V_{x_2} = -\int_{-w_2/2}^{w_2/2}\int_{x_2}^{b_1/2}\sigma_{P_2}(x,y)dxdy \quad (12)$$

$$V_{x_2} = \frac{6M_{y2}{x_2}^2}{{b_1}^3} + \frac{P_2x_2}{b_1} - \frac{P_2b_1 + 3M_{y2}}{2b_1} \quad (13)$$

Taking into account that the derived of the moment is the shear force is presented as follows

$$V_{x_2} = \frac{dM_{y_2'}}{dx_2} \quad (14)$$

where: $M_{y2'}$ is the moment around the axis "y_2'" and V_{x2} is the shear force at a distance "x_2".

Now substituting Eq. (13) into Eq. (14) and integrating to obtain the moment in term of "x_2", this is presented as follows

$$M_{y_2'} = \frac{2M_{y2}{x_2}^3}{{b_1}^3} + \frac{P_2{x_2}^2}{2b_1} - \frac{P_2x_2}{2} - \frac{3M_{y2}x_2}{2b_1} + C_2 \quad (15)$$

Substituting "$x_2 = b_1/2$" and $M_{y2'} = 0$ into Eq. (15), the constant "C_2" is obtained

$$C_2 = \frac{P_2b_1}{8} + \frac{M_{y2}}{2} \quad (16)$$

Now, substituting Eq. (16) into Eq. (15), the equation of moments is

$$M_{y_2'} = \frac{P_2(2x_2 - b_1)^2}{8b_1} + \frac{M_{y2}\left(4{x_2}^3 - 3{b_1}^2x_2 + {b_1}^3\right)}{2{b_1}^3} \quad (17)$$

Substituting "$x_2 = c_2/2$" into Eq. (17) to obtain "$M_{b'}$", this is

$$M_{b'} = \frac{\left[P_2{b_1}^2 + 2M_{y2}(2b_1 + c_2)\right](b_1 - c_2)^2}{8{b_1}^3} \quad (18)$$

2.2.1.3 Moment around the axis x_1'- x_1' of $y_s - c_2/2 \le y_1 \le y_s$

The shear force "V_{y1}" is found through the volume of pressure the area formed by the axis x_1'- x_1' with a width "a_1" and the free end (top side of the Fig. 2) of the footing

$$V_{y_1} = -\int_{y_1}^{y_s}\int_{-a_1/2}^{a_1/2}\sigma(x,y)dxdy \quad (19)$$

$$V_{y_1} = \frac{M_{xT}a_1{y_1}^2}{2I_x} + \frac{Ra_1y_1}{A} - \frac{2RI_xa_1y_s + M_{xT}Aa_1{y_s}^2}{2AI_x} \quad (20)$$

Considering that the derived of the moment is the shear force is obtained

$$V_{y_1} = \frac{dM_{x_1'}}{dy_1} \quad (21)$$

where: $M_{x1'}$ is the moment around the axis "x_1'" and V_{y1} is the shear force at a distance "y_1".

Now substituting Eq. (20) into Eq. (21) and integrating to obtain the moment in term of "x_2", this is presented as follows

$$M_{x_1'} = \frac{M_{xT}a_1{y_1}^3}{6I_x} + \frac{Ra_1{y_1}^2}{2A} - \frac{Ra_1y_sy_1}{A} - \frac{M_{xT}a_1{y_s}^2y_1}{2I_x} + C_3 \quad (22)$$

Substituting "$y_1 = y_s$" and $M_{x1'} = 0$ into Eq. (22), the constant "C_3" is found

$$C_3 = \frac{Ra_1{y_s}^2}{2A} + \frac{M_{xT}a_1{y_s}^3}{3I_x} \quad (23)$$

Now, substituting Eq. (23) into Eq. (22), the equation of moments is

$$M_{x_1'} = \frac{Ra_1(y_1 - y_s)^2}{2A} + \frac{M_{xT}a_1({y_1}^3 - 3{y_s}^2y_1 + 2{y_s}^3)}{6I_x} \quad (24)$$

Substituting "$y_1 = y_s - c_2/2$" into Eq. (24), the moment $M_{c2/2}$ (Moment in the column center 1) is

$$M_{c_2/2'} = \frac{[6RI_x + M_{xT}A(6y_s - c_2)]a_1{c_2}^2}{48AI_x} \quad (25)$$

2.2.1.4 Moment around the axis x_1'- x_1' of $y_s - a_2 \le y_1 \le y_s - c_2/2$

Shear force "V_{y1}" is found through the volume of pressure the area formed by the axis x_1'- x_1' with a width "a_1" and the free end (top side of the Fig. 2) of the footing

$$V_{y_1} = P_1 - \int_{y_1}^{y_s}\int_{-a_1/2}^{a_1/2}\sigma(x,y)dxdy \quad (26)$$

$$V_{y_1} = P_1 + \frac{M_{xT}a_1{y_1}^2}{2I_x} + \frac{Ra_1y_1}{A} - \frac{2RI_xa_1y_s + M_{xT}Aa_1{y_s}^2}{2AI_x} \quad (27)$$

The moment by Eq. (21) is presented

$$M_{x_1'} = P_1 y_1 + \frac{M_{xT} a_1 {y_1}^3}{6I_x} + \frac{R a_1 {y_1}^2}{2A} - \frac{R a_1 y_s y_1}{A} - \frac{M_{xT} a_1 {y_s}^2 y_1}{2I_x} + C_4 \quad (28)$$

Substituting "$y_1 = y_s - c_2/2$" and $M_{c_2/2'} = \frac{[6RI_x + M_{xT} A(6y_s - c_2)] a_1 {c_2}^2}{48AI_x} - M_{x1}$ into Eq. (28), the constant "C_4" is obtained

$$C_4 = \frac{a_1 {y_s}^2 (3RI_x + 2M_{xT} A y_s) - 3P_1 AI_x (2y_s - c_2)}{6AI_x} - M_{x1} \quad (29)$$

Now, substituting Eq. (29) into Eq. (28) the equation of moments is

$$M_{x_1'} = \frac{P_1(2y_1 - 2y_s + c_2)}{2} + \frac{R a_1 (y_1 - y_s)^2}{2A} + \frac{M_{xT} a_1 ({y_1}^3 - 3{y_s}^2 y_1 + 2{y_s}^3)}{6I_x} - M_{x1} \quad (30)$$

Substituting "$y_1 = y_s - c_2$" into Eq. (30), the moment $M_{c'}$ is

$$M_{c'} = \frac{c_2\{a_1 c_2[3RI_x + M_{xT} A(3y_s - c_2)] - 3P_1 AI_x\}}{6AI_x} - M_{x1} \quad (31)$$

Substituting "$y_1 = y_s - a_2$" " into Eq. (30), the moment $M_{d'}$ is

$$M_{d'} = \frac{a_1 {a_2}^2 [3RI_x + M_{xT} A(3y_s - a_2)]}{6AI_x} - \frac{P_1(2a_2 - c_2)}{2} - M_{x1} \quad (32)$$

2.2.1.5 Moment around the axis

x_2'- x_2' of $y_s - (L + c_2/2 - b_2/2) \le y_2 \le y_s - a_2$

Shear force "V_{y2}" is found through the volume of pressure the area formed by the axis x_2'- x_2' with a width "c" and the free end (top side of the Fig. 2) of the footing

$$V_{y_2} = P_1 - \int_{y_s - a_2}^{y_s} \int_{-a_1/2}^{a_1/2} \sigma(x,y)\,dx\,dy - \int_{y_2}^{y_s - a_2} \int_{-c/2}^{c/2} \sigma(x,y)\,dx\,dy \quad (33)$$

$$V_{y_2} = P_1 + \frac{M_{xT} c {y_2}^2}{2I_x} + \frac{R c y_2}{A} - \frac{R[a_1 a_2 + c(y_s - a_2)]}{A} - \frac{M_{xT}[a_1 {y_s}^2 - (a_1 - c)(y_s - a_2)^2]}{2I_x} \quad (34)$$

The moment by Eq. (21) is obtained

$$M_{x_2'} = -\frac{M_{xT}[a_1 {y_s}^2 - (a_1 - c)(y_s - a_2)^2] y_2}{2I_x} + P_1 y_2 - \frac{R[a_1 a_2 + c(y_s - a_2)] y_2}{A} + \frac{R c {y_2}^2}{2A} + \frac{M_{xT} c {y_2}^3}{6I_x} + C_5 \quad (35)$$

Substituting "$y_2 = y_s - a_2$" and $M_{d'} = \frac{a_1 {a_2}^2 [3RI_x + M_{xT} A(3y_s - a_2)] - 3P_1 AI_x (2a_2 - c_2)}{6AI_x} - M_{x1}$ into Eq. (35), the constant "C_5" is obtained

$$C_5 = \frac{M_{xT}[2a_1 {y_s}^3 - 2(a_1 - c)(y_s - a_2)^3]}{6I_x} + \frac{R[a_1 a_2 (2y_s - a_2) + c(y_s - a_2)^2]}{2A} - \frac{P_1(2y_s - c_2)}{2} - M_{x1} \quad (36)$$

Now, substituting Eq. (36) into Eq. (35), the equation of moments is

$$M_{x_2'} = -\frac{M_{xT}(a_1 - c)(y_s - a_2)^2 (2y_s - 2a_2 - 3y_2)}{6I_x} + \frac{M_{xT}[a_1 {y_s}^2 (2y_s - 3y_2) + c {y_2}^3]}{6I_x} + \frac{R[a_1 a_2 (2y_s - 2y_2 - a_2)]}{2A} + \frac{R[c(y_2 - y_s + a_2)^2]}{2A} + \frac{P_1(2y_2 - 2y_s + c_2)}{2} - M_{x1} \quad (37)$$

If the Eq. (34) is made equal to zero ($V_{y2} = 0$), the position of the axis *e*'-*e*' in the interval "$y_s - (L + c_2/2 - b_2/2) \le y_2 = y_m \le y_s - a_2$" is obtained, this is the position of the maximum moment.

The shear force is presented at a distance "y_m", therefore "y_2" is substituted by "y_m" into Eq. (34), and the position is shown as follows

$$y_m = \pm\sqrt{\frac{[RI_x + M_{xT} A(y_s - a_2)]^2}{{M_{xT}}^2 A^2} + \frac{2RI_x a_1 a_2}{M_{xT} Ac} + \frac{a_1 a_2 (2y_s - a_2)}{c} - \frac{2P_1 I_x}{M_{xT} c}} - \frac{RI_x}{M_{xT} A} \quad (38)$$

If "y_2" is made equal to "y_m" into Eq. (37), and Eq. (38) is substituted into Eq. (37) the maximum moment should be obtained.

Substituting "$y_2 = y_s - (L + c_2/2 - b_2/2)$" into Eq. (37), the moment $M_{f'}$ is

$$M_{f'} = \frac{M_{xT} a_1 a_2 (a_2 - 2y_s)[2y_s - 3(2L + c_2 - b_2)]}{12I_x} + \frac{Rc(L - a_2 - b_2/2 + c_2/2)^2}{2A} + \frac{Ra_1 a_2 (2L - a_2 - b_2 + c_2)}{2A} - \frac{P_1(2L - b_2)}{2} - \frac{M_{xT} c y_s (y_s - a_2)^2}{6I_x} + \frac{M_{xT} c (y_s - a_2)^2 (2L + c_2 - b_2)}{4I_x} + \frac{M_{xT} c[y_s - (L + c_2/2 - b_2/2)]^3}{6I_x} + \frac{M_{xT} a_2 (a_1 - c)(y_s - a_2)^2}{3I_x} - M_{x1} \quad (39)$$

2.2.1.6 Moment around the axis x_3'- x_3' of $y_s - (L + c_2/2) \leq y_3 \leq y_s - (L + c_2/2 - b_2/2)$

Shear force "V_{y3}" is found through the volume of pressure the area formed by the axis x_3'- x_3' with a width "b_1" and the free end (top side of the Fig. 2) of the footing

$$V_{y_3} = P_1 - \int_{y_3}^{y_s-(L+c_2/2-b_2/2)} \int_{-b_1/2}^{b_1/2} \sigma(x,y)dxdy - \int_{y_s-(L+c_2/2-b_2/2)}^{y_s-a_2} \int_{-c/2}^{c/2} \sigma(x,y)dxdy - \int_{y_s-a_2}^{y_s} \int_{-a_1/2}^{a_1/2} \sigma(x,y)dxdy \quad (40)$$

$$V_{y_3} = \frac{M_{xT} b_1 {y_3}^2}{2I_x} - \frac{M_{xT}(b_1-c)(2y_s-2L-c_2+b_2)^2}{8I_x} - \frac{M_{xT}[a_1{y_s}^2-(a_1-c)(y_s-a_2)^2]}{2I_x} - \frac{R(b_1-c)(2y_s-2L-c_2+b_2)}{2A} - \frac{R[a_1a_2+c(y_s-a_2)]}{A} + \frac{Rb_1y_3}{A} + P_1 \quad (41)$$

The moment by Eq. (21) is obtained

$$M_{x_3'} = P_1y_3 - \frac{M_{xT}(b_1-c)(2y_s-2L-c_2+b_2)^2y_3}{8I_x} + \frac{M_{xT}(a_1-c)(y_s-a_2)^2y_3}{2I_x} + \frac{Rb_1{y_3}^2}{2A} - \frac{R[a_1a_2+c(y_s-a_2)]y_3}{A} - \frac{R(b_1-c)(2y_s-2L-c_2+b_2)y_3}{2A} - \frac{M_{xT}a_1{y_s}^2y_3}{2I_x} + \frac{M_{xT}b_1{y_3}^3}{6I_x} + C_6 \quad (42)$$

Substituting "$y_3 = y_s - (L + c_2/2 - b_2/2)$" and $M_{f'} = \frac{R[c(L-a_2-b_2/2+c_2/2)^2+a_1a_2(2L-a_2-b_2+c_2)]}{2A} - \frac{P_1(2L-b_2)}{2} + \frac{M_{xT}\{[a_1a_2(a_2-2y_s)-c(y_s-a_2)^2][y_s-3(L+c_2/2-b_2/2)]\}}{6I_x} + \frac{M_{xT}\{c[y_s-(L+c_2/2-b_2/2)]^3+2a_2(a_1-c)(y_s-a_2)^2\}}{6I_x} - M_{x1}$ into Eq. (42), the constant "C_6" is obtained

$$C_6 = \frac{M_{xT}[a_1{y_s}^3+(a_2-y_s)(a_1-c)(y_s-a_2)^2]}{3I_x} + \frac{M_{xT}(b_1-c)[2y_s-2L-c_2+b_2]^3}{24I_x} + \frac{Ra_1a_2(2y_s-a_2)}{2A} + \frac{Rc(y_s-a_2)^2}{2A} + \frac{R(b_1-c)[2y_s-(2L+c_2-b_2)]^2}{8A} - \frac{P_1(2y_s-c_2)}{2} - M_{x1} \quad (43)$$

Now, substituting Eq. (43) into Eq. (42), the equation of moments is

$$M_{x_3'} = -\frac{M_{xT}(b_1-c)[y_s-(L+c_2/2-b_2/2)]^2y_3}{2I_x} + \frac{M_{xT}(a_2-y_s)(a_1-c)(y_s-a_2)^2}{3I_x} + \frac{M_{xT}(b_1-c)[2y_s-2L-c_2+b_2]^3}{24I_x} + \frac{M_{xT}(a_1-c)(y_s-a_2)^2y_3}{2I_x} - \frac{M_{xT}a_1{y_s}^2(3y_3-2y_s)}{6I_x} + \frac{M_{xT}b_1{y_3}^3}{6I_x} + \frac{Rb_1{y_3}^2}{2A} - \frac{R[a_1a_2+c(y_s-a_2)]y_3}{A} - \frac{R(b_1-c)[2y_s-2L-c_2+b_2]y_3}{2A} + \frac{R[a_1{y_s}^2-(a_1-c)(y_s-a_2)^2]}{2A} + \frac{R(b_1-c)[2y_s-2L-c_2+b_2]^2}{8A} + \frac{P_1(2y_3-2y_s+c_2)}{2} - M_{x1} \quad (44)$$

Substituting "$y_3 = y_s - (L + c_2/2 - c_4/2)$" into Eq. (44), the moment $M_{g'}$ is

$$M_{g'} = \frac{M_{xT}(a_1-c)(y_s-a_2)^2(4a_2+2y_s-6L-3c_2+3c_4)}{12I_x} + \frac{M_{xT}a_1{y_s}^2(6L-2y_s+3c_2-3c_4)}{12I_x} + \frac{M_{xT}b_1(2y_s-2L-c_2+c_4)^3}{48I_x} + \frac{M_{xT}(b_1-c)(2L-2y_s+c_2-b_2)^2(b_2-c_4)}{16I_x} + \frac{M_{xT}(b_1-c)(2L-2y_s+c_2-b_2)^3}{48I_x} + \frac{Ra_1a_2(2L-a_2+c_2-c_4)}{2A} - \frac{P_1(2L-c_4)}{2} + \frac{Rc(y_s-a_2)(2L-y_s-a_2+c_2-c_4)}{2A} - \frac{R(b_1-c)(2L-2y_s+c_2-b_2)^2}{8A} - \frac{R(b_1-c)(2L-2y_s+c_2-b_2)(b_2-c_4)}{4A} + \frac{Rb_1(2y_s-2L-c_2+c_4)^2}{2A} - M_{x1} \quad (45)$$

Substituting "$y_3 = y_s - (L + c_2/2)$" into Eq. (44), the moment $M_{c4/2'}$ (Moment in the column center 2) is

$$M_{\frac{c_4}{2}'} = \frac{M_{xT}(a_1-c)(y_s-a_2)^2(4a_2+2y_s-6L-3c_2)}{12I_x} + \frac{M_{xT}a_1{y_s}^2(3L-y_s+3c_2/2)}{6I_x} + \frac{M_{xT}(b_1-c)(2L-2y_s+c_2-b_2)^3}{48I_x} + \frac{M_{xT}b_2(b_1-c)(2L-2y_s+c_2-b_2)^2}{16I_x} \quad (46)$$

$$+\frac{M_{xT}b_1(2y_s-2L-c_2)^3}{6I_x}+\frac{Ra_1a_2(2L-a_2+c_2)}{2A}+\frac{Rc(y_s-a_2)(2L-y_s-a_2+c_2)}{2A}-\frac{R(b_1-c)\left[(L-y_s+c_2/2)^2-{b_2}^2/4\right]}{2A}+\frac{Rb_1(2y_s-2L-c_2)^2}{8A}-P_1L-M_{x1} \quad (46)$$

2.2.1.7 Moment around the axis x_3'- x_3' of $y_s - b \le y_4 \le y_s - (L + c_2/2)$

Shear force "V_{y3}" is found through the volume of pressure the area formed by the axis x_4'- x_4' with a width "b_1" and the free end (top side of the Fig. 2) of the footing

$$V_{y_4}=P_1+P_2-\int_{y_4}^{y_s-(L+c_2/2-b_2/2)}\int_{-b_1/2}^{b_1/2}\sigma(x,y)dxdy-\int_{y_s-(L+c_2/2-b_2/2)}^{y_s-a_2}\int_{-c/2}^{c/2}\sigma(x,y)dxdy-\int_{y_s-a_2}^{y_s}\int_{-a_1/2}^{a_1/2}\sigma(x,y)dxdy \quad (47)$$

$$V_{y_4}=-\frac{M_{xT}(b_1-c)[y_s-(L+c_2/2-b_2/2)]^2}{2I_x}-\frac{M_{xT}[a_1{y_s}^2-(a_1-c)(y_s-a_2)^2]}{2I_x}-\frac{R(b_1-c)(2y_s-2L-c_2+b_2)}{2A}-\frac{R[a_1a_2+c(y_s-a_2)]}{A}+\frac{Rb_1y_4}{A}+\frac{M_{xT}b_1{y_4}^2}{2I_x}+P_1+P_2 \quad (48)$$

The moment by Eq. (21) is obtained

$$M_{x_4'}=Ry_4-\frac{M_{xT}(b_1-c)(2y_s-2L-c_2+b_2)^2y_4}{2I_x}+\frac{M_{xT}(a_1-c)(y_s-a_2)^2y_4}{2I_x}+\frac{Rb_1{y_4}^2}{2A}-\frac{R[a_1a_2+c(y_s-a_2)]y_4}{A}-\frac{R(b_1-c)(2y_s-2L-c_2+b_2)y_4}{2A}-\frac{M_{xT}a_1{y_s}^2y_4}{2I_x}+\frac{M_{xT}b_1{y_4}^3}{6I_x}+C_7 \quad (49)$$

Substituting "$y_4 = y_s - (L + c_2/2)$" and $M_{c_4/2'} = \frac{Rb_1[y_s-(L+c_2/2)]^2}{2A}+\frac{R[a_1a_2(2L-a_2+c_2)+c(y_s-a_2)(2L-y_s-a_2+c_2)]}{2A}-\frac{R(b_1-c)\left[(L-y_s+c_2/2)^2-{b_2}^2/4\right]}{2A}+\frac{M_{xT}b_1[y_s-(L+c_2/2)]^3}{6I_x}+\frac{M_{xT}\{a_1{y_s}^2(3L-y_s+3c_2/2)+(a_1-c)(y_s-a_2)^2(2a_2+y_s-3L-3c_2/2)\}}{6I_x}+\frac{M_{xT}(b_1-c)[y_s-(L+c_2/2-b_2/2)]^2(L-y_s+c_2/2+b_2)}{6I_x}-P_1L-M_{x1}-M_{x2}$ into Eq. (49), the constant "C_7" is obtained

$$C_7=\frac{M_{xT}(b_1-c)(2y_s-2L-c_2+b_2)^3}{24I_x}+\frac{M_{xT}a_1{y_s}^3}{3I_x}+\frac{M_{xT}(a_2-y_s)(a_1-c)(y_s-a_2)^2}{3I_x}+\frac{R[a_1{y_s}^2-(a_1-c)(y_s-a_2)^2]}{2A}+\frac{R(b_1-c)(2y_s-2L-c_2+b_2)^2}{8A}-\frac{R(2y_s-c_2)}{2}-P_2L-M_{x1}-M_{x2} \quad (50)$$

Now, substituting Eq. (50) into Eq. (49), the equation of moments is

$$M_{x_4'}=\frac{M_{xT}b_1{y_4}^3}{6I_x}-\frac{M_{xT}(b_1-c)(2y_s-2L-c_2+b_2)^2y_4}{8I_x}+\frac{M_{xT}(a_2-y_s)(a_1-c)(y_s-a_2)^2}{3I_x}+\frac{M_{xT}(b_1-c)(2y_s-2L-c_2+b_2)^3}{24I_x}+\frac{M_{xT}a_1{y_s}^3}{3I_x}+\frac{M_{xT}(a_1-c)(y_s-a_2)^2y_4}{2I_x}+\frac{Rb_1{y_4}^2}{2A}-\frac{R[a_1a_2+c(y_s-a_2)]y_4}{A}-\frac{R(b_1-c)(2y_s-2L-c_2+b_2)y_4}{2A}+\frac{R[a_1{y_s}^2-(a_1-c)(y_s-a_2)^2]}{2A}+\frac{R(b_1-c)(2y_s-2L-c_2+b_2)^2}{8A}+\frac{R(2y_4-2y_s+c_2)}{2}-\frac{M_{xT}a_1{y_s}^2y_4}{2I_x}+P_2L-M_{x1}-M_{x2} \quad (51)$$

Substituting "$y_4 = y_s - (L + c_2/2 + c_4/2)$" into Eq. (51), the moment $M_{h'}$ is

$$M_{h'}=\frac{M_{xT}(a_1-c)(y_s-a_2)^2(4a_2+2y_s-6L-3c_2-3c_4)}{12I_x}+\frac{M_{xT}a_1{y_s}^2(6L-2y_s+3c_2+3c_4)}{12I_x}+\frac{M_{xT}b_1(2y_s-2L-c_2-c_4)^3}{48I_x}+\frac{M_{xT}(b_1-c)(2L-2y_s+c_2-b_2)^2(c_4+b_2)}{16I_x}+\frac{M_{xT}(b_1-c)(2L-2y_s+c_2-b_2)^3}{48I_x}+\frac{Ra_1a_2(2L-a_2+c_2+c_4)}{2A}-\frac{P_1(2L+c_4)}{2}-\frac{P_2c_4}{2}+\frac{Rc(y_s-a_2)(2L-y_s-a_2+c_2+c_4)}{2A}-\frac{R(b_1-c)(2L-2y_s+c_2-b_2)^2}{4A}-\frac{R(b_1-c)(2L-2y_s+c_2-b_2)(c_4+b_2)}{4A}+\frac{Rb_1(2y_s-2L-c_2-c_4)^2}{8A}-M_{x1}-M_{x2} \quad (52)$$

2.2.2 Bending shear (unidirectional shear force)

Critical sections for bending shear are obtained at a distance "d" starting the junction of the column with the footing as seen in Fig. 3, these are presented in sections i'-i', j'-j', k'-k', l'-l', m'-m', n'-n' and o'-o'.

2.2.2.1 Bending shear on axis i'-i'

Substituting "$x_1 = c_1/2 + d$" into Eq. (6) to obtain the bending shear "$V_{fi'}$" on the axis i'-i' of the footing, this is

$$V_{fi'} = -\frac{[P_1 {a_1}^2 + 3M_{y1}(a_1 + c_1 + 2d)](a_1 - c_1 - 2d)}{2{a_1}^3} \quad (53)$$

2.2.2.2 Bending shear on axis j'-j'

Substituting "$x_2 = c_3/2 + d$" into Eq. (13) to obtain the bending shear "V_{fj}" on the axis j'-j' of the footing, this is

$$V_{fj'} = -\frac{[P_2 {b_1}^2 + 3M_{y2}(b_1 + c_3 + 2d)](b_1 - c_3 - 2d)}{2{b_1}^3} \quad (54)$$

2.2.2.3 Bending shear on axis k'-k' (If $y_1 \geq y_s - a_2$)

Substituting "$y_1 = y_s - c_2 - d$" into Eq. (27) to obtain the bending shear "V_{fk}" on the axis k'-k' of the footing, this is

$$V_{fk'} = P_1 - \frac{[2RI_x + M_{xT}A(2y_s - c_2 - d)]a_1(c_2 + d)}{2AI_x} \quad (55)$$

2.2.2.4 Bending shear on axis l'-l'

Substituting "$y_1 = y_s - a_2$" into Eq. (27) or Eq. (34) to obtain the bending shear "$V_{fl'}$" on the axis l'-l' of the footing, this is

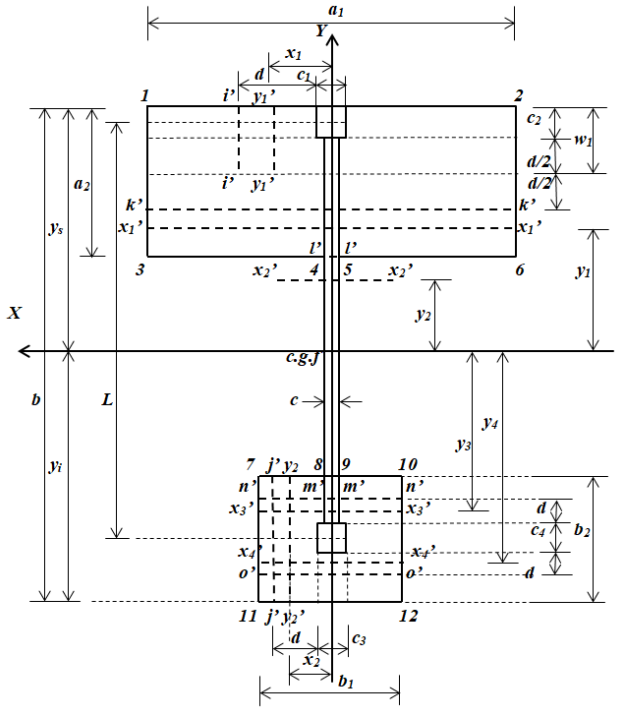

Fig. 3 Critical sections for bending shear

$$V_{fl'} = P_1 - \frac{[2RI_x + M_{xT}A(2y_s - a_2)]a_1a_2}{2AI_x} \quad (56)$$

2.2.2.5 Bending shear on axis k'-k' (If $y_2 \leq y_s - a_2$)

Substituting "$y_2 = y_s - c_2 - d$" into Eq. (34) to obtain the bending shear "$V_{fk'}$" on the axis k'-k' of the footing, this is

$$V_{fk'} = \frac{M_{xT}c(a_2 - c_2 - d)(2y_s - a_2 - c_2 - d)}{2I_x} - \frac{M_{xT}a_1a_2(2y_s - a_2)}{2I_x} + P_1 - \frac{R[a_1a_2 - c(a_2 - c_2 - d)]}{A} \quad (57)$$

2.2.2.6 Bending shear on axis n'-n' (If $y_2 \geq y_s - L - c_2/2 + b_2/2$)

Substituting "$y_2 = y_s - (L + c_2/2 - c_4/2 - d)$" into Eq. (34) to obtain the bending shear "$V_{fn'}$" on the axis n'-n' of the footing, this is

$$V_{fn'} = P_1 - \frac{R[a_1a_2 - c(a_2 - L - c_2/2 + c_4/2 + d)]}{A} - \frac{M_{xT}[a_1{y_s}^2 - (a_1 - c)(y_s - a_2)^2]}{2I_x} + \frac{M_{xT}c(2y_s - 2L - c_2 + c_4 + d)^2}{8I_x} \quad (58)$$

2.2.2.7 Bending shear on axis m'-m'

Substituting "$y_2 = y_s - (L + c_2/2 - b_2/2)$" into Eq. (34) or Eq. (41) to obtain the bending shear "$V_{fm'}$" on the axis m'-m' of the footing, this is

$$V_{fm'} = P_1 + \frac{Rc[2y_s - 2L - c_2 + b_2]}{2A} - \frac{R[a_1a_2 + c(y_s - a_2)]}{A} - \frac{M_{xT}[a_1{y_s}^2 - (a_1 - c)(y_s - a_2)^2]}{2I_x} + \frac{M_{xT}c(2y_s - 2L - c_2 + b_2)^2}{8I_x} \quad (59)$$

2.2.2.8 Bending shear on axis n'-n' (If $y_3 \leq y_s - L - c_2/2 + b_2/2$)

Substituting "$y_3 = y_s - (L + c_2/2 - c_4/2 - d)$" into Eq. (41) to obtain the bending shear "$V_{fn'}$" on the axis n'-n' of the footing, this is

$$V_{fn'} = P_1 - \frac{M_{xT}(b_1 - c)(2y_s - 2L - c_2 + b_2)^2}{8I_x} - \frac{M_{xT}[a_1{y_s}^2 - (a_1 - c)(y_s - a_2)^2]}{2I_x} + \frac{M_{xT}b_1(2y_s - 2L - c_2 + c_4 + d)^2}{8I_x} + \frac{Rb_1(2y_s - 2L - c_2 + c_4 + d)}{2A} - \frac{R[a_1a_2 + c(y_s - a_2)]}{A} - \frac{R(b_1 - c)(2y_s - 2L - c_2 + b_2)}{2A} \quad (60)$$

2.2.2.9 Bending shear on axis *o*'-*o*'

Substituting "$y_4 = y_s - (L + c_2/2 + c_4/2 + d)$" into Eq. (48) to obtain the bending shear "V_{fo}" on the axis *o*'-*o*' of the footing, this is

$$V_{fo'} = P_1 + P_2 - \frac{M_{xT}(b_1 - c)(2y_s - 2L - c_2 + b_2)^2}{8I_x} - \frac{M_{xT}[a_1 y_s{}^2 - (a_1 - c)(y_s - a_2)^2]}{2I_x} + \frac{M_{xT} b_1 (2y_s - 2L - c_2 - c_4 - d)^2}{8I_x} + \frac{Rb_1(2y_s - 2L - c_2 - c_4 - d)}{2A} - \frac{R[a_1 a_2 + c(y_s - a_2)]}{A} - \frac{R(b_1 - c)(2y_s - 2L - c_2 + b_2)}{2A} \quad (61)$$

2.2.3 Punching shear (*bidirectional shear force*)

Critical section for the punching shear appears at a distance "*d*/2" starting the junction of the column with the footing in the two directions, as shown in Fig. 4.

2.2.3.1 Punching shear for column 1

Critical section for the punching shear is presented in rectangular section formed by points 13, 14, 15 and 16. Punching shear acting on the footing "V_{p1}" is the force "P_1" acting on column 1 subtracting the pressure volume of the area formed by the points 13, 14, 15 and 16

$$V_{p1} = P_1 - \int_{y_s-(c_2+d/2)}^{y_s} \int_{-(c_1+d)/2}^{(c_1+d)/2} \sigma(x,y)dxdy \quad (62)$$

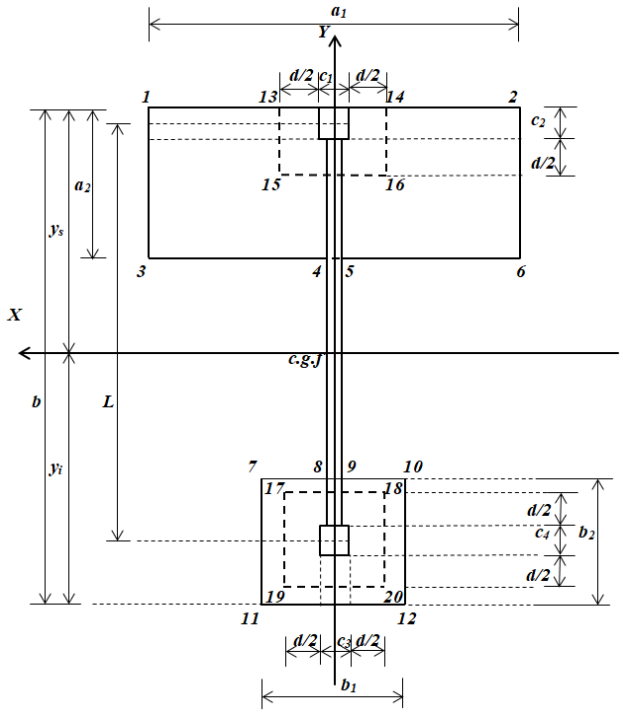

Fig. 4 Critical sections for the punching shear

$$V_{p1} = P_1 - \frac{[2RI_x + M_{xT}A(2y_s - c_2 - d/2)](c_1 + d)(c_2 + d/2)}{2AI_x} \quad (63)$$

2.2.3.2 Punching shear for column 2

The critical section for the punching shear is presented in rectangular section formed by points 17, 18, 19 and 20. Punching shear acting on the footing "V_{p2}" is the force "P_2" acting on column 2 subtracting the pressure volume of the area formed by the points 17, 18, 19 and 20

$$V_{p2} = P_2 - \int_{y_s-(L+c_2/2-c_4/2-d/2)}^{y_s-(L+c_2/2+c_4/2+d/2)} \int_{-(c_3+d)/2}^{(c_3+d)/2} \sigma(x,y)dxdy \quad (64)$$

$$V_{p2} = P_2 - \left[\frac{[2RI_x + M_{xT}A(2y_s - 2L - c_2)](c_3 + d)(c_4 + d)}{2AI_x}\right] \quad (65)$$

3. Numerical example

The design of a strap combined footing supporting two square columns is presented in Fig. 2, with the information following: the two columns are of 40×40 *cm*; L = 8.00 *m*; H = 2.0 *m*; P_{D1} = 600 *kN*; P_{L1} = 400 *kN*; M_{Dx1} = 160 *kN-m*; M_{Lx1} = 140 *kN-m*; M_{Dy1} = 120 *kN-m*; M_{Ly1} = 80 *kN-m*; P_{D2} = 300 *kN*; P_{L2} = 200 *kN*; M_{Dx2} = 80 *kN-m*; M_{Lx2} = 70 *kN-m*; M_{Dy2} = 120 *kN-m*; M_{Ly2} = 80 *kN-m*; f'_c = 35 *MPa*; f_y = 420 *MPa*; q_a = 250 *kN/m*^{2}; γ_{ppz} = 24 *kN/m*^{3}; γ_{pps} = 15 *kN/m*^{3}. Where: H is the depth of the footing, P_D is the dead load, P_L is the live load, M_{Dx} is the moment around the axis "*X*-*X*" of the dead load, M_{Lx} is the moment around the axis "*X*-*X*" of the live load, M_{Dy} is the moment around the axis "*Y*-*Y*" of the dead load, M_{Ly} is the moment around the axis "*Y*-*Y*" of the live load.

The loads and moments acting on soil are: P_1 = 1000 *kN*; M_{x1} = 300 *kN-m*; M_{y1} = 200 *kN-m*; P_2 = 500 *kN*; M_{x2} = 150 *kN-m*; M_{y2} = 200 *kN-m*.

The thickness of the footing is proposed, the first proposal is the minimum thickness of 25 cm in accordance with regulations of the ACI, and subsequently the thickness is revised to satisfy the following conditions: moments, bending shear, and punching shear. If such conditions are not satisfied, is proposed a greater thickness until it fulfills the three conditions mentioned. The thickness of the footing than fulfills the three conditions listed above is 90 *cm* (effective depth is 82 *cm*, and coating is 8 *cm*), the available load capacity of the soil "σ_{adm}" is 211.90 *kN/m*^{2} (Gambhir 2008, González-Cuevas and Robles-Fernandez-Villegas 2005, McCormac and Brown 2013, Luévanos-Rojas *et al.* 2013, Luévanos-Rojas 2014a, b, 2015).

Substituting the values of "σ_{adm} = 211.90 *kN/m*^{2}, L = 8.00 *m*, P_1 = 1000 *kN*, M_{x1} = 300 *kN-m*, M_{y1} = 200 *kN-m*, P_2 = 500 *kN*, M_{x2} = 150 *kN-m*, M_{y2} = 200 *kN-m*, $a_1 \geq$ 1.00 *m*, $a_2 \geq$ 1.00 *m*, $b_1 \geq$ 1.00 *m*, $b_2 \geq$ 1.00 *m*, c = 0.40 *m* and 8.20 + b_2/2 = b" in Eqs. (26) to (42) of Part 1 and using the MAPLE-15 software are obtained: A_{tmin} = 10.15 *m*^{2}, I_x = 93.31 *m*^{4}, I_y = 19.00 *m*^{4}, y_s = 2.57 *m*, M_{xT} = 0.00 *kN-m*, M_{yT} = 400 *kN-m*, R = 1500 *kN*, a_1 = 6.09 *m*, a_2 = 1.00 *m*, b = 8.86 *m*, b_1 = 1.10

m, b_2 = 1.31 m, c = 0.40 m, σ_1 = 211.09 kN/m^2, σ_2 = 83.69 kN/m^2, σ_3 = 211.90 kN/m^2, σ_4 = 152.01 kN/m^2, σ_5 = 143.59 kN/m^2, σ_6 = 83.69 kN/m^2, σ_7 = 159.36 kN/m^2, σ_8 = 152.01 kN/m^2, σ_9 = 143.59 kN/m^2, σ_{10} = 136.23 kN/m^2, σ_{11} = 159.36 kN/m^2, σ_{12} = 136.23 kN/m^2.

Table 1 The bending shear forces

Analysis section axis	Shear force acting kN	Allowable shear force kN	Width of analysis m
i'-*i*'	−511.99	567.81	0.81
j'-*j*'	0*	855.22	1.22
l'-*l*'	131.28**	280.40	0.40
k'-*k*'	113.61	280.40	0.40
n'-*n*'	−362.10	280.40	0.40
m'-*m*'	−382.22**	280.40	0.40
o'-*o*'	0*	771.10	1.10

* The axis falls outside of the footing
** The axes that join the beam and the footing

Therefore the practical dimensions of the strap combined footing supporting two square columns are: a_1 = 6.10 m, a_2 = 1.00 m, b = 8.90 m, b_1 = 1.10 m, b_2 = 1.40 m, c = 0.40 m.

Substituting the values of a_1 = 6.10 m, a_2 = 1.00 m, b = 8.90 m, b_1 = 1.10 m, b_2 = 1.40 m and c = 0.40 m in the same MAPLE-15 software are found: A_{tmin} = 10.24 m^2, I_x = 96.12 m^4, I_y = 19.11 m^4, y_s = 2.61 m, M_{xT} = 65.23 kN-m, M_{yT} = 400 kN-m, R = 1500 kN, a_1 = 6.10 m, a_2 = 1.00 m, b = 8.90 m, b_1 = 1.10 m, b_2 = 1.40 m, c = 0.40 m, σ_1 = 212.11 kN/m^2, σ_2 = 84.40 kN/m^2, σ_3 = 211.43 kN/m^2, σ_4 = 151.76 kN/m^2, σ_5 = 143.39 kN/m^2, σ_6 = 83.72 kN/m^2, σ_7 = 154.68 kN/m^2, σ_8 = 147.35 kN/m^2, σ_9 = 138.98 kN/m^2, σ_{10} = 131.65 kN/m^2, σ_{11} = 153.73 kN/m^2, σ_{12} = 130.70 kN/m^2.

The factored mechanical elements (P, M_x, M_y) acting on the footing are: $P_{u1} = 1.2P_{D1} + 1.6P_{L1}$ = 1360 kN; $M_{ux1} = 1.2M_{Dx1} + 1.6M_{Lx1}$ = 416 kN-m; $M_{uy1} = 1.2M_{Dy1} + 1.6M_{Ly1}$ = 272 kN-m; $P_{u2} = 1.2P_{D2} + 1.6P_{L2}$ = 680 kN; $M_{ux2} = 1.2M_{Dx2} + 1.6M_{Lx2}$ = 208 kN-m; $M_{uy2} = 1.2M_{Dy2} + 1.6M_{Ly2}$ = 272 kN-m.

Table 2 Reinforcement steel of the New Model

Reinforcement steel				Area cm^2
Footing 1	Direction of the axis "Y"	Steel at the top with a width of $a_1 - c$	Temperature steel	92.34
			Steel proposed	96.33(19Ø1") Spacing 32.11 *cm*
		Steel in the bottom with a width of $a_1 - c$	Temperature steel	92.34
			Steel proposed	96.33(19Ø1") Spacing 32.11 *cm*
	Direction of the axis "X"	Steel at the top with a width of a_2	Temperature steel	16.20
			Steel proposed	20.28(4Ø1") Spacing 25.00 *cm*
		Steel at the bottom with a width of w_1	Main steel	34.43
			Minimum steel	22.14
			Steel proposed	35.49(7Ø1") Spacing 11.93 *cm*
		Steel at the bottom with a width of $a_2 - w_1$	Temperature steel	3.08
			Steel proposed	3.96(2Ø5/8") Spacing 11.93 *cm*
Strap beam		Steel at the top with a width of c	Main steel	31.27
			Minimum steel	10.93
			Steel proposed	35.49(7Ø1")
		Steel in the bottom with a width of c	Temperature steel	6.48
			Steel proposed	10.14(2Ø1")
		Shear reinforcement steel with a width of c	Stirrups to a spacing of 36.5 cm	A_v = 1.27(1Ø1/2")
Footing 2	Direction of the axis "Y"	Steel at the top with a width of b_1	Temperature steel	17.82
			Steel proposed	20.28(4Ø1") Spacing 30.5 *cm*
		Steel in the bottom with a width of b_1	Temperature steel	17.82
			Steel proposed	20.28(4Ø1") Spacing 30.5 *cm*
	Direction of the axis "X"	Steel at the top with a width of b_2	Temperature steel	22.68
			Steel proposed	25.35(5Ø1") Spacing 28.00 *cm*
		Steel at the bottom with a width of w_2	Main steel	3.33
			Minimum steel	33.35
			Steel proposed	35.49(7Ø1") Spacing 17.43 *cm*
		Steel at the bottom with a width of $b_2 - w_2$	Temperature steel	2.92
			Steel proposed	3.96(2Ø5/8") Spacing 9.00 *cm*

4. Results

Substituting the factored mechanical elements into Eqs. (15)-(16) of the part 1 are obtained: M_{xT} = 100.72 *kN-m*; M_{yT} = 544 *kN-m*.

Now, substituting the corresponding values to obtain the moments acting on critical sections of the strap combined footing are shown: $M_{a'}$ = 1028.10 *kN-m*; $M_{b'}$ = 102.95 *kN-m*; $M_{c'}$ = −589.51 *kN-m*; $M_{d'}$ = −889.11 *kN-m*; $M_{e'}$ = −903.88 *kN-m*; $M_{f'}$ = −63.95 *kN-m*; $M_{g'}$ = −47.50 *kN-m*; $M_{h'}$ = 22.38 *kN-m*. The maximum moment "$M_{e'}$" is presented in y_m = −0.03 *m*.

The effective depth to the maximum moment of the axes parallel to the axis "*X-X*" is: *d* = 53.90 *cm*. The effective depth to the maximum moment of the axes parallel to the axis "*Y-Y*" is: *d* = 40.40 *cm* (column 1), and *d* = 10.42 *cm* (column 2). The effective depth after performing different proposals is: *d* = 82.00 *cm*, *r* = 8.00 *cm*, *t* = 90.00 *cm*.

Table 1 shows the bending shear forces acting on critical sections of the strap combined footing.

Now, substituting the corresponding values to obtain the punching shear forces acting on critical sections of the strap combined footing are presented: V_{p1} = 1160.85 *kN*; V_{p2} = 615.13 *kN*. The punching shear resisted by the concrete to "V_{p1}" are $\emptyset_v V_{cp1}$ = 5972.49 *kN*, $\emptyset_v V_{cp1}$ = 10363.36 *kN*, $\emptyset_v V_{cp1}$ = 3864.55 *kN*, and to "V_{p2}" are $\emptyset_v V_{cp2}$ = 4626.58 *kN*, $\emptyset_v V_{cp2}$ = 9925.28 *kN*, $\emptyset_v V_{cp2}$ = 2993.67 *kN*. Therefore, the two conditions are accepted.

The reinforcement steel for the strap combined footing is shown in Table 2.

The minimum development length for deformed bars appears in Table 3. The reinforcement steel hooks are not needed in the two directions.

Fig. 5 shows the dimensions and the reinforcement steel of the strap combined footing.

Effects that govern the design for the strap combined footings are the moments, bending shear, and punching shear with regard to thickness of the concrete footings, and the reinforcement steel is governed by the moments.

Substituting $c = b_1$ in the equations for moments and shear forces of this document are obtained the equations for the T-shaped combined footings. Now, substituting $a = a_1 = b_1 = c$ and $b = a_2 = b_2$ in the equations for moments and shear forces of this document are obtained the equations for the rectangular combined footings.

A way to validate the new model is as follows: For the interval "$y_s - b \leq y_4 \leq y_s - (L + c_2/2)$" is substituted "$y_4 = y_s - b$" into Eq. (51), the moment acting on footing is M_{x4} = 0 *kN-m*. For the interval "$y_s - b \leq y_4 \leq y_s - (L + c_2/2)$" is substituted "$y_4 = y_s - b$" into Eq. (48), the bending shear force acting on footing is V_{y4} = 0 *kN*.

Therefore the new model in this paper is valid, because the equilibrium of the moments and the loads acting on the footing against the pressure exerted by the ground on the footing are verified.

Table 3 Development length

Concept	Steel at the top	Steel in the bottom
ψ_t	1.3	1.0
$\psi_e = \lambda$	1.0	1.0
l_d (*cm*)	178.02	110.85
l_a(*cm*)	264.00(O.K.)	285.00(O.K.)

Where: l_d is the development length, l_a is the available length

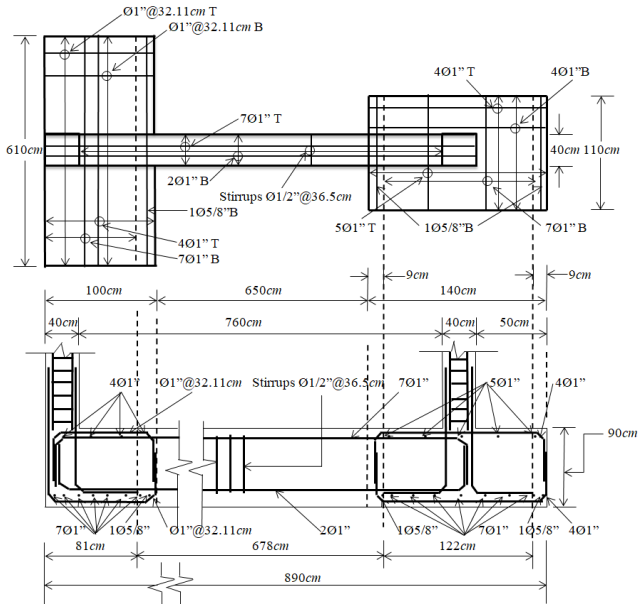

Fig. 5 Diagram for the strap combined footing

5. Conclusions

The new model presented in this paper applies only for design of the strap combined footings, the structural member assumes that should be rigid and the supporting soil layers elastic, which meet expression of the bidirectional bending, i.e., the variation of pressure is linear.

The presented new model at this paper is concluded the following:

(1) The thicknesses for the new model of the strap combined footings are governed by the bending shear, and the isolated footings are governed by the punching shear.
(2) The new model is not limited with respect to the classic model that considers an axial load and a moment around the axis "X" (transverse axis) applied to each column, i.e., the resultant force from the applied loads is located on the axis "Y" (longitudinal axis), and its position must match with the geometric center of the footing.
(3) The new model is adjusted to real conditions with respect to the classical model, because the new model taking into account the soil real pressure and the classical model considers the maximum pressure in all the contact surface, when the axial load and moments in two directions to each column are presented.
(4) The new model for design of foundations subject to axial load and moments in two directions to each column considers one or two property lines

restricted.

The new model presented in this paper for the structural design of the strap combined footings subjected to an axial load and moment in two directions in each column, also it can be applied to others cases: (1) The footings subjected to a concentric axial load in each column, (2) The footings subjected to an axial load and moment in one direction in each column.

The main advantage of this document is that it can be used for rectangular and T-shaped combined footings.

The suggestions for future research, when is presented another type of soil, by example in totally cohesive soils (clay soils) and totally granular soils (sandy soils), the pressure diagram is not linear and should be treated differently (see Fig. 1).

Acknowledgments

The research described in this paper was financially supported by the Institute of Multidisciplinary Researches of the Faculty of Accounting and Administration of the Autonomous University of Coahuila. The authors also gratefully acknowledge the helpful comments and suggestions of the reviewers, which have improved the presentation.

References

ACI 318S-14 (American Concrete Institute) (2014), Building Code Requirements for Structural Concrete and Commentary, Committee 318.

Agrawal, R. and Hora, M.S. (2012), "Nonlinear interaction behaviour of infilled frame-isolated footings-soil system subjected to seismic loading", *Struct. Eng. Mech., Int. J.*, **44**(1), 85-107.

Anil, Ö, Akbaş, S.O., BabagĪray, S., Gel, A.C. and Durucan, C. (2017), "Experimental and finite element analyses of footings of varying shapes on sand", *Geomech. Eng., Int. J.*, **12**(2), 223-238.

Bowles, J.E. (2001), *Foundation Analysis and Design*, McGraw-Hill, New York, NY, USA.

Calavera-Ruiz, J. (2000), *Calculo de Estructuras de Cimentación*, Intemac Ediciones, México.

Chen, W-R., Chen, C-S and Yu, S-Y. (2011), "Nonlinear vibration of hybrid composite plates on elastic foundations", *Struct. Eng. Mech., Int. J.*, **37**(4), 367-383.

Cure, E., Sadoglu, E., Turker, E. and Uzuner, B.A. (2014), "Decrease trends of ultimate loads of eccentrically loaded model strip footings close to a slope", *Geomech. Eng., Int. J.*, **6**(5), 469-485.

Das, B.M., Sordo-Zabay, E. and Arrioja-Juarez, R. (2006), *Principios de ingeniería de cimentaciones*, Cengage Learning Latín América, México.

Dixit, M.S. and Patil, K.A. (2013), "Experimental estimate of Nγ values and corresponding settlements for square footings on finite layer of sand", *Geomech. Eng., Int. J.*, **5**(4), 363-377.

ErzÍn, Y. and Gul, T.O. (2013), "The use of neural networks for the prediction of the settlement of pad footings on cohesionless soils based on standard penetration test", *Geomech. Eng., Int. J.*, **5**(6), 541-564.

Gambhir, M.L. (2008), *Fundamentals of Reinforced Concrete Design*, Prentice-Hall, of India Private Limited.

Gere, J.M. and Goodno, B.J. (2009), *Mecánica de Materiales*, Cengage Learning, México.

González-Cuevas, O.M. and Robles-Fernández-Villegas, F. (2005), *Aspectos fundamentales del concreto reforzado*, Limusa, México.

Guler, K. and Celep, Z. (2005), "Response of a rectangular plate-column system on a tensionless Winkler foundation subjected to static and dynamic loads", *Struct. Eng. Mech., Int. J.*, **21**(6), 699-712.

Khatri, V.N., Debbarma, S.P., Dutta, R.K. and Mohanty, B. (2017), "Pressure-settlement behavior of square and rectangular skirted footings resting on sand", *Geomech. Eng., Int. J.*, **12**(4), 689-705.

López-Chavarría, S., Luévanos-Rojas, A. and Medina-Elizondo, M. (2017), "A new mathematical model for design of square isolated footings for general case", *Int. J. Innov. Comput. I.*, **13**(4), 1149-1168.

Luévanos-Rojas, A. (2014a), "Design of isolated footings of circular form using a new model", *Struct. Eng. Mech., Int. J.*, **52**(4), 767-786.

Luévanos-Rojas, A. (2014b), "Design of boundary combined footings of rectangular shape using a new model", *Dyn.*, **81**(188), 199-208.

Luévanos-Rojas, A. (2015), "Design of boundary combined footings of trapezoidal form using a new model", *Struct. Eng. Mech., Int. J.*, **56**(5), 745-765.

Luévanos-Rojas, A. (2016a), "A comparative study for the design of rectangular and circular isolated footings using new models", *Dyn.*, **83**(196), 149-158.

Luévanos-Rojas, A. (2016b), "Un nuevo modelo para diseño de zapatas combinadas rectangulares de lindero con dos lados opuestos restringidos", *Revista Alconpat*, **6**(2), 172-187.

Luévanos-Rojas, A., Faudoa-Herrera, J.G., Andrade-Vallejo, R.A. and Cano-Alvarez M.A. (2013), "Design of Isolated Footings of Rectangular Form Using a New Model", *Int. J. Innov. Comput. I.*, **9**(10), 4001-4022.

Luévanos-Rojas, A., Barquero-Cabrero, J.D., López-Chavarría, S. and Medina-Elizondo, M. (2017), "A comparative study for design of boundary combined footings of trapezoidal and rectangular forms using new models", *Coupled Syst. Mech., Int. J.*, **6**(4), 417-437.

Luévanos-Rojas, A., López-Chavarría, S. and Medina-Elizondo, M. (2018), "A new model for T-shaped combined footings Part II: Mathematical model for design", *Geomech. Eng., Int. J.*, **14**(1), 61-69.

Maheshwari, P. and Khatri, S. (2012), "Influence of inclusion of geosynthetic layer on response of combined footings on stone column reinforced earth beds", *Geomech. Eng., Int. J.*, **4**(4), 263-279.

McCormac, J.C. and Brown, R.H. (2013), *Design of Reinforced Concrete*, John Wiley & Sons, New York, NY, USA.

Mohamed, F.M.O., Vanapalli, S.K. and Saatcioglu, M. (2013), "Generalized Schmertmann Equation for settlement estimation of shallow footings in saturated and unsaturated sands", *Geomech. Eng., Int. J.*, **5**(4), 363-377.

Mohebkhah, A. (2017), "Bearing capacity of strip footings on a stone masonry trench in clay", *Geomech. Eng., Int. J.*, **13**(2), 255-267.

Orbanich, C.J. and Ortega, N.F. (2013), "Analysis of elastic foundation plates with internal and perimetric stiffening beams on elastic foundations by using Finite Differences Method", *Struct. Eng. Mech., Int. J.*, **45**(2), 169-182.

Orbanich, C.J., Dominguez, P.N. and Ortega, N.F. (2012), "Strenghtening and repair of concrete foundation beams whit fiber composite materials", *Mater. Struct.*, **45**, 1693-1704.

Rad, A.B. (2012), "Static response of 2-D functionally graded circular plate with gradient thickness and elastic foundations to

compound loads", *Struct. Eng. Mech., Int. J.*, **44**(2), 139-161.
Shahin, M.A. and Cheung, E.M. (2011), "Stochastic design charts for bearing capacity of strip footings", *Geomech. Eng., Int. J.*, **3**(2), 153-167.
Smith-Pardo, J.P. (2011), "Performance-based framework for soil-structure systems using simplified rocking foundation models", *Struct. Eng. Mech., Int. J.*, **40**(6), 763-782.
Tomlinson, M.J. (2008), *Cimentaciones, Diseño y Construcción*, Trillas, México.
Uncuoğlu, E. (2015), "The bearing capacity of square footings on a sand layer overlying clay", *Geomech. Eng., Int. J.*, **9**(3), 287-311.
Zhang, L., Zhao, M.H., Xiao, Y. and Ma, B.H. (2011), "Nonlinear analysis of finite beam resting on Winkler with consideration of beam-soil interface resistance effect", *Struct. Eng. Mech., Int. J.*, **38**(5), 573-592.

CC